1. Toufik Ahmed HOUARI[1], 2. Omar DAHOU[1], 3. Youcef Islam DJILANI KOBIBI[1], 4. Hocine BOUCHEKARA[1]

University Mustapha Stambouli of Mascara, Algeria (1)
ORCID: 1. 0000-0003-0494-9056; 2. 0000-0003-1698-9338; 3. 0000-0001-6772-8838

doi:10.15199/48.2023.04.22

Modeling the performance of an Electrodynamic screen (EDS) with artificial intelligence techniques

Abstract. *Artificial neural networks by their learning, classification, and decision capabilities, have contributed in the development of several fields. In electrostatics and its applications, neural networks are used to solve the problems of modeling, diagnosis and control of different modes of operation of machines. This work focuses on the application of artificial neural networks for modeling the operation of a three-phase electric field electrodynamic screen for moving micronized polyvinyl chloride (PVC) particles, with an average particle size of 250 µm. The neural network used is a multilayer perceptron type network, trained by the gradient back propagation algorithm. The input vector contains parameters taken from the studied experimental device: applied voltage U [kV], frequency [Hz] and diameter d [mm]. The output vector contains the mass of the product collected at the output of the electrodynamic screen.*

Streszczenie. *plSztuczne sieci neuronowe dzięki swoim zdolnościom uczenia się, klasyfikacji i podejmowania decyzji przyczyniły się do rozwoju kilku dziedzin. W elektrostatyce i jej zastosowaniach sieci neuronowe są wykorzystywane do rozwiązywania problemów modelowania, diagnozowania i sterowania różnymi trybami pracy maszyn. W pracy skupiono się na zastosowaniu sztucznych sieci neuronowych do modelowania działania ekranu elektrodynamicznego trójfazowego pola elektrycznego dla poruszających się cząstek mikronizowanego polichlorku winylu (PVC) o średniej wielkości cząstek 250 µm. Wykorzystywana sieć neuronowa jest wielowarstwową siecią typu perceptron, wytrenowaną przez algorytm wstecznej propagacji gradientu. Wektor wejściowy zawiera parametry zaczerpnięte z badanego urządzenia doświadczalnego: przyłożone napięcie U [kV], częstotliwość [Hz] i średnicę d [mm]. Wektor wyjściowy zawiera masę produktu zebraną na wyjściu ekranu elektrodynamicznego.(* (***Modelowanie wydajności ekranu elektrodynamicznego (EDS) za pomocą technik sztucznej inteligencji)***

Keywords: Electrodynamic screen (EDS), travelling waves, artificial neural networks, modeling,
Słowa kluczowe: Ekran elektrodynamiczny (EDS), fale biegnące, sztuczne sieci neuronowe, modelowanie,

Introduction

The use of a non-uniform electric field for manipulation of dielectric particles is gaining attention in various research and industrial fields, These applications include separation and sorting [1, 2, 3, 4-34], trapping and assembly [1, 35,36], patterning [36-41], purification [42, 43], and characterization [44-46] of micro/nano particles as well as the development of nanostructured electronic and optical devices [47-51].

Indeed, the mechanical processes used present many problems, they are expensive, energy consuming and less flexible; this has led researchers to develop new techniques that feature electrostatic forces that can offer a more efficient alternative. One promising electrostatic device is the so-called electric curtain. It consists of a series of parallel electrodes deposited on a dielectric surface and supplied with a multiphase electric potential [52]. In this system, if the electric field is high enough, the Coulomb force can overcome the attractive forces such as the gravitational force, the image force and the adhesion force, and leads to the motion of the particles. Masuda [53-55] was one of the first researchers to develop and study this system. He undertook a series of experimental and theoretical studies to investigate the behavior of particles in the seventies and eighties of the last century. One of the first applications of this system was in the field of electro photography for the supply of toner to printers [56]. In the last fifteen years, thanks to the development of thin film deposition technology that allows us to deposit transparent electrodes on transparent substrate; many research groups have been interested in using the electric curtain technique to develop the so-called electrodynamic screen (EDS) [57]. This system is used for dust removal from photovoltaic panels and solar collectors. Indeed, the accumulation of dust and sand on photovoltaic systems can greatly reduce their efficiency; traditional systems such as washing and brushing consume a huge amount of water and energy and damage the photovoltaic collectors. Work in this area has shown promising results under both terrestrial and extraterrestrial conditions [58,59]. The effect of forces such as Coulomb force, dielectrophoretic force, image force, adhesion force, drag force, and gravity, on the motion of particles has been extensively studied in many research works. The study of the force balance is essential to determine the particle motion; however, a more detailed study is needed for a more complete understanding of some experimentally observed particle behaviors such as the direction of the particle motion [59]. The objective of our work is to deepen this study by introducing artificial intelligence for the modeling and optimization of the operation of this electrodynamic moving wave screen, this will allow us to achieve the maximum efficiency of this process. This study is composed of two parts: The first part is an experimental study where we analyze the efficiency of the electrodynamic screens for the displacement of particles of micrometer size as a function of frequency, the value of applied voltage, and the inter-electrode distance. The second part consists of a numerical study in which artificial neural networks are used to predict the recovery of the displaced particles as a function of different electrical and mechanical parameters. For this purpose, the characteristics of a moving wave electrodynamic screen will be modeled using an artificial neural network (ANN). In order to optimize its operation, the particle swarm optimization (PSO) method was chosen, which has the advantage of being efficient on a wide range of problems, without requiring the user to modify the basic structure of the algorithm.

Material and methods

An ECB comprising 3 phases has been developed, using an electronic PCB board plate, of dimensions 190 × 150 mm^2 , on which were drawn parallel copper electrodes of 1 mm width and 90 mm length (Figure 3). Five models were developed corresponding to three different inter-electrodes spacing d (0.5, 0.625, 0.75, 0.875, and 1 mm)(figure 1). An insulating adhesive tape film covers the conveyor to minimise the risk of breakdown sparks between electrodes. The AC voltage square signals applied to the conveyor electrodes were visualised using a storage digital oscilloscope (Gwinstek GDS-3154).

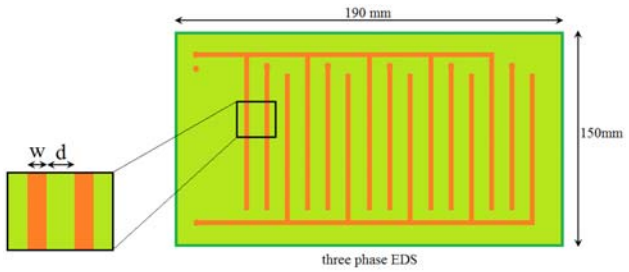

Fig. 1. The three-phase electrodynamic screen (EDS) used

A homemade three-phase compact power supply was used in the present work. The developed 3-phase AC power supply delivers a voltage up to 1000 V and a variable frequency of several kHz. The power supply includes a DC/HVDC converter of 1 kV, which is then converted into three rectangular shape voltages with a phase shift of 120°.

The same sample of micronized PVC particles with an average particle size of 250 microns, prepared with a vibrating sieve machine, was used for all the experiments in this work. Each sample of mass m=500 mg was deposited as a monolayer on the same rectangular portion of the conveyor (figure 2). At the end of each experiment, the mass of the particles swept from the electrodynamic screen was recovered and weighed using a 1 mg precision electronic balance (Kern, ALG 220-4NM).

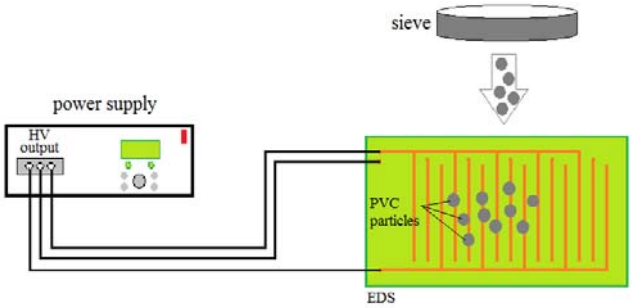

Fig. 2. Descriptive schematic of the experimental setup

PMC modeling process

The modeling of particle displacement by the travelling wave technique using the artificial neural network method is done according to the flowchart presented in figure 3:

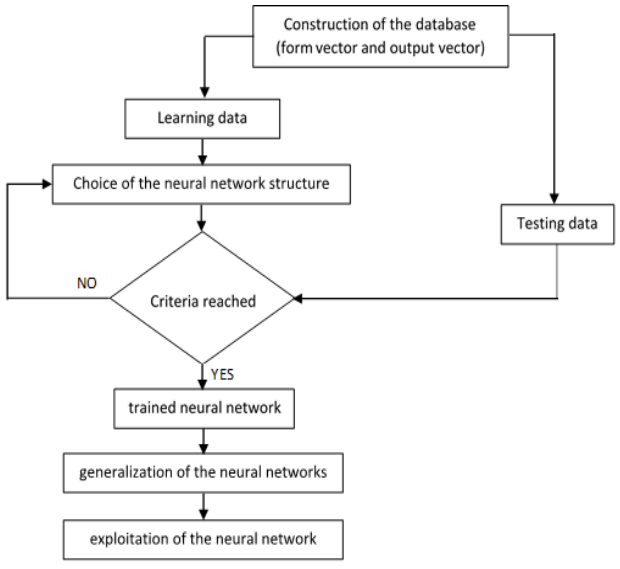

Fig.3. PMC modeling flowchart.

Construction of the vector

In this step, we collect (record) the output corresponding to the different states of the studied device (Voltage, Frequency and inter-electrode distance) for 5 variation levels. These 4 parameters form the vectors (matrix) of the learning base and the network test.

Learning and testing the network:

One part of the database is used to train the network, and the other is used to test it. The training consists in looking for an optimal configuration of the network parameters (weights, bias, etc.) corresponding to a high success rate. Once the network has been trained, we still need to perform tests in order to verify that our network reacts correctly.

Operation of the network

After the optimal network configuration is determined, the network becomes capable of predicting other experimental results.

PMC implementation in MATLAB

Experimental study

In order to carry out the experiments on the displacement of the particles, it is essential to know the parameters that influence the displacement of the PVC particles,

The range of variation of the controllable factors that we have chosen in our work, namely the applied voltage U, the frequency f and the distance inter electrodes is summarized in the table below:

Table 1. study domain

study domain		
Factor	min	max
Frequency f [Hz]	10	50
Voltage U [V]	300	1000
distance inter electrodes d [mm]	0.5	1

In order to carry out our experimental study, a cyclical procedure must be followed:

Preparation

- set the weight of the PVC at 500 mg.
- distribute the PVC on the surface of the electrodynamic screen.
- set the frequency (10, 20, 30, 40, 50 Hz)
- connect the electrodynamic screen to the HV generator.

Application

- start the generator and then adjust the voltage (300, 474, 650, 825, 1000 V) with the start of the stopwatch at the same time, the time is limited in (60 s).
- Once the cleaning process is finished, we remove the PVC on the sides of the electrodynamic screen and weigh it in order to have the yield of the displaced PVC mass (%).

Neural Network Architecture and Implementation

There are currently more than 50 types of networks used in different applications. In the present work we are particularly interested in feed-forward networks. Figure.4 shows the connections between the neurons of this structure.

Recent research gives more interest to the use of sigmoid functions which are generally used as activation functions in the neural network.

There are three steps in the construction of a ANN, the training, testing and validation performed by the network. Typically, by random sampling method, about 70% of experimental data are used for training, 15% for validation and the rest of the data for testing - The best performance of the architecture is defined by the coefficient of

determination (R^2) which defines the integrity of the experimental data:

(1) $$R^2 = 1 - \frac{\sum_{i=1}^{n}(t_i - y_i)^2}{\sum_{i=1}^{n}(y_i)^2}$$

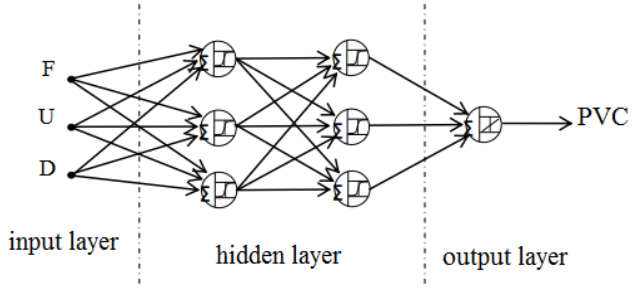

Fig. 4. Feed-forward neural network model

The network is then tested to evaluate the accuracy of the prediction by a measure of the mean square error (MSE), which is determined by:

(2) $$MSE = \frac{\sum_{i=1}^{n}(t_i - y_i)^2}{n}$$

In the present study, the neural network is configured as a multiple input single output (MISO) model in the MATLAB environment.

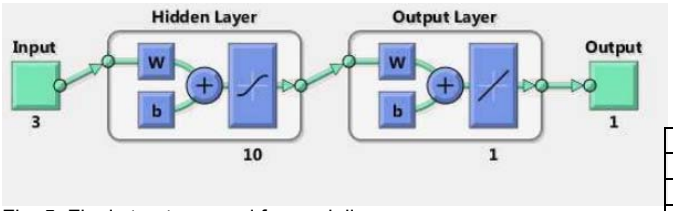

Fig. 5. Final structure used for modeling

Our network is trained from the experimental data. All these values will then be normalized to centered reduced values (between -1 and 1) to ensure the stability of the result

Results and discussion

Training of the RNA network

The learning (or training) performance of our ANN is given in Fig. 6. The X axis represents the measured values (Y_measured) and the Y axis represents the predictions (Y_predicted). The blue line indicates the bisector, equality between measured and predicted values All values are normalized between -1 and 1.

The best performance of the ANN architecture is determined by a mean square error, (abbreviated MSE in the rest of the work) close to 0, and by a maximum coefficient of determination (abbreviated R^2 in the rest of the work) close to 1.

Figure.6 shows an alignment, with a small dispersion, of the graph points on the first bisector. This tells us that the model predicts exactly the response of the real process but only in the experimental points of the learning base. On the other hand, the dispersion is due to the representation of all the points (experimental+test+validation). The model thus obtained must be adjusted on all the points. The efficiency of the network would be improved with the number of hidden neurons and the optimal percentage of the data in the three steps:

% train : Percentage of data in the learning stage
% test : Percentage of data in the test step
% valid: Percentage of data in the validation step

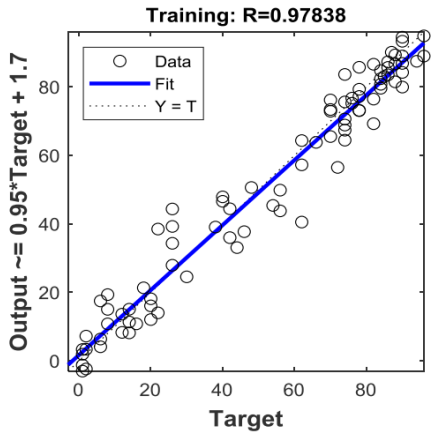

Fig. 6. Training performance of the ANN

Choice of the number of hidden units of the ANN

The number of units in the hidden layer is always important because it is the number of units that determines the optimization and the performance of the expert system. In this section, we will study the influence of the choice of this parameter on the classification performance of a multilayer perceptron. The most obvious method currently used in the exact determination of the number of layers and the number of neurons consists in applying a trial-and-error strategy to determine the structure of the best performing network. We vary the number of neurons in the hidden layer from 10 to 100 and perform several trials (total of 3 trials) for each number of hidden neurons. The objective is to minimize the mean square error MSE to obtain an R^2 indicator as close as possible to 1 (100%).

Table 2. Variation of the number of hidden neurons

number of neurons	**MSE**	**R^2**
10	9.70093 E-3	9.61769 E-1
20	4.93376 E-2	8.50737 E-1
30	1.02092 E-1	2.56431 E-1
40	1.10545 E-1	7.17358 E-1
50	3.15603 E-1	7.17358 E-1
60	8.18370 E-1	7.38301 E-1
70	4.67158 E-1	7.43582 E-1
80	2.27801 E-1	3.18665 E-2
90	1.73326	3.67013 E-1
100	1.22373	1.21895 E-1

The Figure (7) Shows the performance of our ANN for a variation in the number of neurons, the Percentage of data is respectively 15% for the test and 15% for the validation.

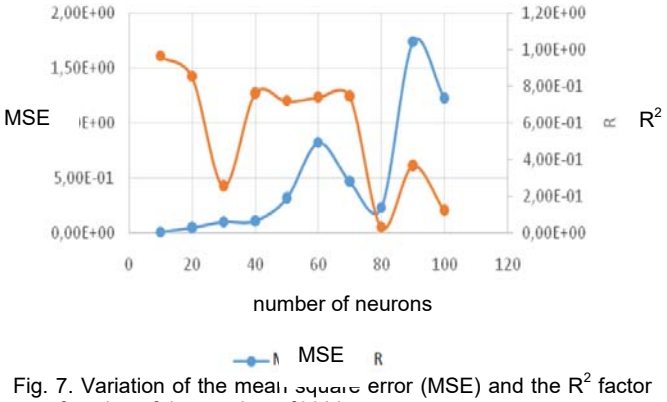

Fig. 7. Variation of the mean square error (MSE) and the R^2 factor as a function of the number of hidden neurons

From Table 2, and Figure 7 we can see that the mean square error (MSE) increases with the increase of the number of hidden neurons, while the determination factor

R^2 decreases. The trend shows that a reduced number in the hidden layer produces good results. Thus, the number of hidden neurons is fixed at 10 in the rest of our study.

The evaluation of the mean square error (MSE) between the three types of data in our study, namely train (learning), testing and validation, is represented in Figure 8. We notice that the learning process continues to regress, while the other processes, namely validation and test, stabilize around the best performance found around the 7th epoch, which represents an overlearning of the network. The best performance is reached at the 7th epoch with a value equal to 0.012.

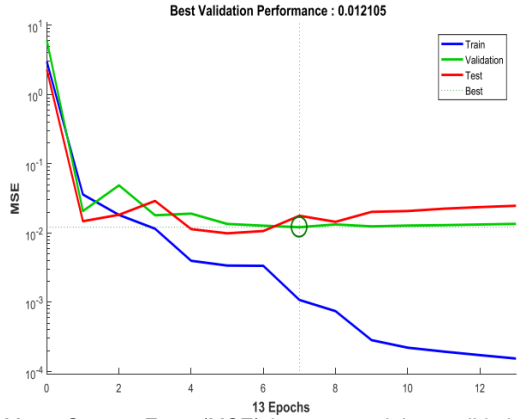

Fig.8. Mean Square Error (MSE) between training, validation and test

Figure 9 shows the value of the determination factor R^2 for the three steps, where it increases from 0.9723 to 0.9967.

Figure 9 shows the regression analysis between the targeted and predicted outcomes of the trained ANN for each phase. The R^2 shows the efficiency of the model in predicting the targeted output in each phase. The performance of the training phase is shown in Figure 9 (a), which shows the highest R^2 of 0.99676 obtained for the training phase. The training data is well predicted because it was also used to train the network. It also shows that a well performing network can be obtained by training the optimal network for the given number of input and output parameters.

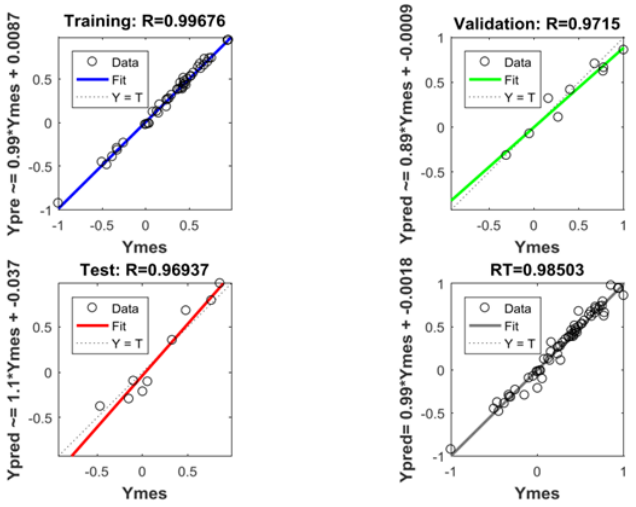

Fig.9. Determination factor (R^2) for learning, validation and testing

Figure 9(b) shows the validation dataset predicted using the trained network with R^2 > 0.97. Figure 9(c) shows the generalization ability of the trained network with a performance shown by R^2 > 0, 96. For different studies in the literature, the effectiveness of the ANN model in the validation and testing phase decreases, resulting in a lower R^2 than the training phase, This may be due to the fact that the test dataset is not included in the training phase. The overall data, which includes the learning, validation, and prediction phase data points, are shown in Figure 9(d) with their ANN model outputs. The overall R^2 is 0.985.

Conclusion

This work was devoted to the experimental approach of the modeling of the operation of a three-phase electrodynamic screen with travelling waves intended for the displacement of the micronized particles in PVC by using the method of the artificial neural networks. We explained this approach step by step. Several parameters participate in the success of this approach such as the parameters of the network; starting with the elements of the input vector (input parameters), passing by the architecture of the network, arriving at the output vector (output parameters). We note here that there are no rules for choosing the parameters of artificial neural networks, but these parameters vary according to the problem studied. Only experience can answer this question. During our tests, we noticed that the increase of the number of neurons in the hidden layer, and consequently the increase of the size of the hidden layer, makes the learning process very slow and influences in a negative way the convergence of the gradient back propagation algorithm. We do not forget the simplicity of implementing a multilayer perceptron neural network under the MATLAB language environment. It is enough to determine the different values corresponding to the different parameters of the network, then to execute the different commands (Newff, train and sim).

REFERENCES

[1] N. G. Green, H. Morgan, and J. J. Milner, Manipulation and trapping of sub-micron bioparticles using dielectrophoresis, *Journal of Biochemical and Biophysical Methods,* 35(1997) , 89-102,

[2] J. Voldman, Electrical forces for microscale cell manipulation, *Annual Review of Biomedical Engineering*, 8(2006), 425-454.

[3] P. R. C. Gascoyne and J. Vykoukal, Particle separation by dielectrophoresis, *Electrophoresis*, 23(2002), 1973-1983.

[4] M. P. Hughes, Strategies for dielectrophoretic separation in laboratory-on-a-chip systems, *Electrophoresis*, 23(2002), 2569-2582.

[5] N. Demierre, T. Braschler, R. Muller, and P. Renaud, Focusing and continuous separation of cells in a microfluidic device using lateral dielectrophoresis, *Sensors and Actuators B-Chemical*, 132(2008), 388-396.

[6] E. M. Nascimento, N. Nogueira, T. Silva, T. Braschler, N. Demierre, P. Renaud, and A. G. Oliva, Dielectrophoretic sorting on a microfabricated flow cytometer: Label free separation of Babesia bovis infected erythrocytes, *Bioelectrochemistry*, 73(2008), 123-128.

[7] T. Yasukawa, M. Suzuki, T. Sekiya, H. Shiku, and T. Matsue, Flow sandwich-type immunoassay in microfluidic devices based on negative dielectrophoresis, *Biosensors & Bioelectronics*, 22(2007), 2730-2736.

[8] J. Auerswald and H. F. Knapp, Quantitative assessment of dielectrophoresis as a micro fluidic retention and separation technique for beads and human blood erythrocytes, *Microelectronic Engineering*, 67(2003), 879-886.

[9] Y. Huang, J. M. Yang, P. J. Hopkins, S. Kassegne, M. Tirado, A. H. Forster, and H. Reese, Separation of simulants of biological warfare agents from blood by a miniaturized dielectrophoresis device, *Biomedical Microdevices*, 5(2003), 217-225.

[10] Z. Y. Wang, O. Hansen, P. K. Petersen, A. Rogeberg, J. P. Kutter, D. D. Bang, and A. Wolff, Dielectrophoresis microsystem with integrated flow cytometers for on-line monitoring of sorting efficiency, *Electrophoresis*, 27(2006), 5081-5092.

[11] J. T. Huang, G. C. Wang, K. M. Tseng, and S. B. Fang, A chip for catching, separating, and transporting bio-particles with dielectrophoresis, *Journal of Industrial Microbiology & Biotechnology*, 35(2008), 1551-1557.

[12] U. Kim, J. R. Qian, S. A. Kenrick, P. S. Daugherty, and H. T. Soh, Multitarget Dielectrophoresis Activated Cell Sorter, *Analytical Chemistry*, 80(2008), 8656-8661.
[13] Y. J. Kang, D. Q. Li, S. A. Kalams, and J. E. Eid, DC-Dielectrophoretic separation of biological cells by size, *Biomedical Microdevices*, 10(2008), 243-249.
[14] G. O. F. Parikesit, A. P. Markesteijn, O. M. Piciu, A. Bossche, J. Westerweel, I. T. Young, and Y. Garini, Size-dependent trajectories of DNA macromolecules due to insulative dielectrophoresis in submicrometer-deep fluidic channels, *Biomicrofluidics*, 2(2008).
[15] R. Krishnan, B. D. Sullivan, R. L. Mifflin, S. C. Esener, and M. J. Heller, Alternating current electrokinetic separation and detection of DNA nanoparticles in high-conductance solutions, *Electrophoresis*, 29(2008), 1765-1774.
[16] J. P. Fu, P. Mao, and J. Y. Han, Nanofilter array chip for fast gel-free biomolecule separation, *Applied Physics Letters*, 87(2005).
[17] H. Morgan, M. P. Hughes, and N. G. Green, Separation of submicron bioparticles by dielectrophoresis, *Biophysical Journal*, 77(1999), 516-525.
[18] I. Ermolina, J. Milner, and H. Morgan, Dielectrophoretic investigation of plant virus particles: Cow Pea Mosaic Virus and Tobacco Mosaic Virus, *Electrophoresis*, 27(2006), 3939-3948.
[19] X. B. Wang, Y. Huang, P. R. C. Gascoyne, and F. F. Becker, Dielectrophoretic manipulation of particles, *Ieee Transactions on Industry Applications*, 33(1997), 660-669.
[20] X. B. Wang, Y. Huang, X. J. Wang, F. F. Becker, and P. R. C. Gascoyne, Dielectrophoretic manipulation of cells with spiral electrodes, *Biophysical Journal*, 72(1997), 1887-1899.
[21] L. L. Jia, S. G. Moorjani, T. N. Jackson, and W. O. Hancock, Microscale transport and sorting by kinesin molecular motors, Biomedical Microdevices, 6(2004), 67-74.
[22] B. H. Lapizco-Encinas, B. A. Simmons, E. B. Cummings, and Y. Fintschenko, Dielectrophoretic concentration and separation of live and dead bacteria in an array of insulators, *Analytical Chemistry*, 76(2004), 1571-1579.
[23] I. F. Cheng, H. C. Chang, and D. Hou, An integrated dielectrophoretic chip for continuous bioparticle filtering, focusing, sorting, trapping, and detecting, *Biomicrofluidics*, 1(2007).
[24] F. Du, M. Baune, A. Kuck, and J. Thoming, Dielectrophoretic Gold Particle Separation, *Separation Science and Technology*, 43(2008), 3842-3855.
[25] M. J. Mendes, H. K. Schmidt, and M. Pasquali, Brownian dynamics simulations of single-wall carbon nanotube separation by type using dielectrophoresis, *Journal of Physical Chemistry* B, 112(2008), 7467-7477.
[26] S. Ozuna-Chacon, B. H. Lapizco-Encinas, M. Rito-Palomares, S. O. Martinez-Chapa, and C. Reyes-Betanzo, Performance characterization of an insulator-based dielectrophoretic microdevice, *Electrophoresis*, 29(2008), 3115-3122.
[27] M. D. Vahey and J. Voldman, An equilibrium method for continuous-flow cell sorting using dielectrophoresis, *Analytical Chemistry*, 80(2008), 3135-3143.
[28] Z. G. Wu, A. Q. Liu, and K. Hjort, Microfluidic continuous particle/cell separation via electroosmotic-flow-tuned hydrodynamic spreading, *Journal of Micromechanics and Microengineering*, 17(2007), 1992-1999.
[29] B. G. Hawkins, A. E. Smith, Y. A. Syed, and B. J. Kirby, Continuous-flow particle separation by 3D insulative dielectrophoresis using coherently shaped, dc-biased, ac electric fields, *Analytical Chemistry*, 79(2007), 7291-7300.
[30] D. F. Chen, H. Du, and W. H. Li, A 3D paired microelectrode array for accumulation and separation of microparticles, *Journal of Micromechanics and Microengineering*, 16(2006), 1162-1169.
[31] J. G. Kralj, M. T. W. Lis, M. A. Schmidt, and K. F. Jensen, Continuous dielectrophoretic size-based particle sorting, *Analytical Chemistry*, 78(2006), 5019- 5025.
[32] M. S. Pommer, Y. T. Zhang, N. Keerthi, D. Chen, J. A. Thomson, C. D. Meinhart, and H. T. Soh, Dielectrophoretic separation of platelets from diluted whole blood in microfluidic channels, *Electrophoresis*, 29(2008), 1213-1218.
[33] S. K. Srivastava, P. R. Daggolu, S. C. Burgess, and A. R. Minerick, Dielectrophoretic characterization of erythrocytes: Positive ABO blood types, *Electrophoresis*, 29(2008), 5033-5046.
[34] D. F. Chen and H. J. Du, A dielectrophoretic barrier-based microsystem for separation of microparticles, *Microfluidics and Nanofluidics*, 3(2007), 603-610.
[35] S. Grilli and P. Ferraro, Dielectrophoretic trapping of suspended particles by selective pyroelectric effect in lithium niobate crystals, *Applied Physics Letters*, 92(2008).
[36] M. Yang and X. Zhang, Electrical assisted patterning of cardiac myocytes with controlled macroscopic anisotropy using a microfluidic dielectrophoresis chip, *Sensors and Actuators a-Physical*, 135(2007), 73-79.
[37] M. Suzuki, T. Yasukawa, H. Shiku, and T. Matsue, Negative dielectrophoretic patterning with colloidal particles and encapsulation into a hydrogel, *Langmuir*, 23(2007), 4088-4094.
[38] A. Rosenthal and J. Voldman, Dielectrophoretic traps for single-particle patterning, *Biophysical Journal*, 88(2005), 2193-2205.
[39] R. Kretschmer and W. Fritzsche, Pearl chain formation of nanoparticles in microelectrode gaps by dielectrophoresis, *Langmuir*, 20(2004), 11797-11801.
[40] D. R. Albrecht, V. L. Tsang, R. L. Sah, and S. N. Bhatia, Photo- and electropatterning of hydrogel-encapsulated living cell arrays, *Lab on a Chip*, 5(2005), 111-118.
[41] L. C. Hsiung, C. H. Yang, C. L. Chiu, C. L. Chen, Y. Wang, H. Lee, J. Y. Cheng, M. C. Ho, and A. M. Wo, A planar interdigitated ring electrode array via dielectrophoresis for uniform patterning of cells, *Biosensors & Bioelectronics*, 24(2008), 869-875.
[42] Z. Chen, Z. Y. Wu, L. M. Tong, H. P. Pan, and Z. F. Liu, Simultaneous dielectrophoretic separation and assembly of single-walled carbon nanotubes on multigap nanoelectrodes and their thermal sensing properties, *Analytical Chemistry*, 78(2006), 8069-8075.
[43] X. M. Liu, J. L. Spencer, A. B. Kaiser, and W. M. Arnold, Selective purification of multiwalled carbon nanotubes by dielectrophoresis within a large array, *Current Applied Physics*, 6(2006), 427-431.
[44] M. P. Hughes, H. Morgan, and F. J. Rixon, Dielectrophoretic manipulation and characterization of herpes simplex virus-1 capsids, *European Biophysics Journal with Biophysics Letters*, 30(2001), 268-272.
[45] S. Basuray and H. C. Chang, Induced dipoles and dielectrophoresis of nanocolloids in electrolytes, *Physical Review E*, 75(2007).
[46] H. B. Li, Y. N. Zheng, D. Akin, and R. Bashir, Characterization and modeling of a microfluidic dielectrophoresis filter for biological species, *Journal of Microelectromechanical Systems*, 14(2005), 103-112.
[47] J. Suehiro, H. Imakiire, S. Hidaka, W. D. Ding, G. B. Zhou, K. Imasaka, and M. Hara, Schottky-type response of carbon nanotube NO2 gas sensor fabricated onto aluminum electrodes by dielectrophoresis, *Sensors and Actuators B-Chemical*, 114(2006), 943-949.
[48] J. Suehiro, G. B. Zhou, and M. Hara, Fabrication of a carbon nanotube-based gas sensor using dielectrophoresis and its application for ammonia detection by impedance spectroscopy, *Journal of Physics D-Applied Physics*, 36(2003), L109-L114.
[49] C. S. Lao, J. Liu, P. X. Gao, L. Y. Zhang, D. Davidovic, R. Tummala, and Z. L. Wang, ZnO nanobelt/nanowire Schottky diodes formed by dielectrophoresis alignment across Au electrodes, *Nano Letters*, 6(2006), 263-266.
[50] S. K. Lee, T. H. Kim, S. Y. Lee, K. C. Choi, and P. Yang, High-brightness gallium nitride nanowire UV-blue light emitting diodes, *Philosophical Magazine*, 87(2007), 2105-2115.
[51] S. Y. Lee, T. H. Kim, D. I. Suh, E. K. Suh, N. K. Cho, W. K. Seong, and S. K. Lee, Dielectrophoretically aligned GaN nanowire rectifiers, *Applied Physics a-Materials Science & Processing*, 87(2007), 739-742.
[52] T.A.Houari, M.E.Zelmat, and A.Tilmatine, Development of a compact power supply for dielectrophoretic applications, *Australian Journal of Electrical and Electronics Engineering*, 18(2021), 172-186.
[53] S. Masuda, K. Fujibayashi, K. Ishida, H. Inaba, Confinement and transport of charged aerosol clouds by means of electric curtain, *The transactions of the Institute of Electrical Engineers of Japan*, 92(1972), 9-18.
[54] S. Masuda, Apparatus for electric field curtain of contact type. U.S. Patent No. 3,778,678. 11 Dec. 1973.
[55] S. Masuda, Booth for electrostatic powder painting with contact type electric field curtain. U.S. Patent No. 3,801,869. 2 Apr. 1974.
[56] A.H.Pohl, K.Pollok et J.S.Crane, Dielectrophoretic force: a comparison of theory and experiment, *Journal of biological physics*, 6(1979), 133-160.
[57] M.N.Horenstein, M.Mazumder et R. Jr, Predecting particle trajectories on an electrodynamic screnn-theory and experiment, *Journal of electrostatics*, 71(2013), 185-188.
[58] H. Pang, P. Atten et JL. Reboud, Dépoussiérage électrostatique pour les particules submicroniques en atmosphère usuelle (Terre) et raréfiée (Planète Mars), University of Joseph Fourier - Grenoble 1, 2006.
[59] A. Zouaghi, N. Zouzou, Numerical modeling of particle motion in traveling wave solar panels cleaning device, *Journal of Electrostatics*, 110(2021).